ACS Catalysis

Research Article

pubs.acs.org/acscatalysis

Cocatalyst Designing: A Regenerable Molybdenum-Containing Ternary Cocatalyst System for Efficient Photocatalytic Water Splitting

G. Wilma Busser,[†] Bastian Mei,[‡] Philipp Weide,[†] Peter C. K. Vesborg,[‡] Kai Stührenberg,[§] Matthias Bauer,[§] Xing Huang,[∥] Marc-Georg Willinger,[∥] Ib Chorkendorff,[‡] Robert Schlögl,[∥] and Martin Muhler*[,†]

[†]Laboratory of Industrial Chemistry, Ruhr-Universität Bochum, Universitätsstraße 150, 44780 Bochum, Germany

[‡]Department of Physics, CINF, Technical University of Denmark, Fysikvej, 2800, Kongens Lyngby, Denmark

[§]Fakultät für Naturwissenschaften, Department Chemie, Universität Paderborn, Warburger Straße 100, 33098 Paderborn, Germany

[∥]Anorganische Chemie, Fritz-Haber-Institut, Faradayweg 4-6, 14195 Berlin, Germany

Supporting Information

ABSTRACT: Earth-abundant materials are required to facilitate upscaling of renewable hydrogen generation. Here, the synthesis of a novel oxidic ternary cocatalyst containing molybdenum, chromium, and copper, which has been found to be highly active in the overall photocatalytic splitting of water over gallium oxide, is described. With the noble metal-free system, requiring hydrogen evolution rates comparable to that of the well-established $Rh_xCr_{2-x}O_3/Ga_2O_3$ water splitting cocatalyst is achieved. Although the stability of the as-prepared ternary cocatalyst system appeared to be poor, the cocatalyst can be easily regenerated and stabilized by an oxygen treatment under ambient conditions. Furthermore, higher MoO_x loadings were found to be more active and showed improved stability. By means of careful characterization using X-ray-based spectroscopy and TEM, the function of the individual cocatalyst compounds was closely examined, suggesting synergetic interactions of molybdena and chromia stabilizing CuO against photoreduction. Although stability issues should be further addressed, this work highlights that multicomponent systems, which are well-studied in industrial processes for heterogeneous reactions and commonly used in various other fields of research, can be used in solar water splitting. In particular, molybdena-containing materials are discovered as a new class of earth-abundant cocatalysts for overall water-splitting.

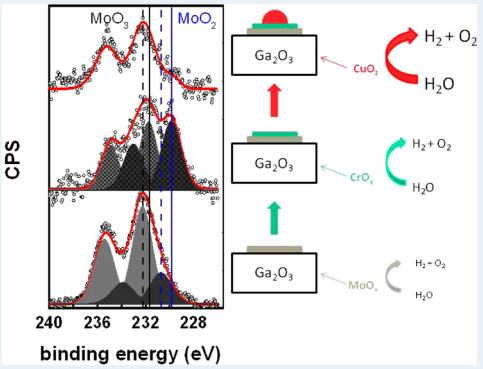

KEYWORDS: *photocatalytic overall water splitting, earth-abundant cocatalyst, sequential photodeposition, back reaction, gallium oxide, molybdenum oxide*

INTRODUCTION

Although the development of new photon-absorbing materials is a major research focus and good progress has been made in the development of materials absorbing large fractions of visible light, most materials suffer from poor hydrogen- and oxygen-evolution capabilities. Because of smaller overpotentials and improved kinetics for catalyzing the hydrogen evolution reaction (HER), noble metals such as Pt,[1,2] Rh,[3] Au[4] and oxides such as RuO_2[5] and $Rh_xCr_{2-x}O_3$[6] are generally used as cocatalysts for photocatalytic hydrogen evolution. Because precious metals are expensive and scarce, it is necessary to explore alternative cocatalysts based on inexpensive and abundant transition metals to facilitate the up-scaling of renewable H_2 production by sunlight-assisted water splitting.[7]

Even though in technical applications, water splitting using powder photocatalysts should preferentially be run under conditions that the H_2 and O_2 concentrations are below the explosion limit (H_2 concentration <4%), it was recently shown by Jaramillo et al.[8] that economical water splitting might be feasible, but a lack of efficient, low-cost photon absorber and cocatalysts hampers its implementation.

Cu-based cocatalysts have gained increasing attention,[9] and recently, we reported on the synthesis of CuO_z/CrO_y-modified Ga_2O_3 by stepwise photodeposition for overall water splitting under UV light irradiation.[10] It was shown that the activity of the CuO_z/CrO_y-modified Ga_2O_3 photocatalyst was highly dependent on the Cu loading, whereas small amounts of CrO_y (0.09 wt % Cr) were sufficient to catalyze the overall reaction. Furthermore, CuO_z/MoO_x-modified Ga_2O_3 showed activities comparable to that of CuO_z/CrO_y-modified Ga_2O_3 (0.2 wt % Cu), suggesting further exploration of the function of MoO_x.[10] In addition, because the overall water splitting rate obtained with a CuO_z/CrO_y-modified Ga_2O_3 photocatalyst is significantly lower compared with $Rh_xCr_{2-x}O_3$-modified Ga_2O_3 photocatalysts,[10] nonnoble-metal-based cocatalysts have to be

Received: May 6, 2015
Published: August 11, 2015

DOI: 10.1021/acscatal.5b01428
ACS Catal. 2015, 5, 5530−5539

improved to be suitable alternatives for the well-established platinum-group metal-based cocatalysts.

For the development of such an efficient and low-cost cocatalyst system, commercially available n-type Ga_2O_3 semiconductors can be used as photon absorber. Ga_2O_3 is known to be able to split water efficiently under UV irradiation upon modification with an appropriate cocatalyst, and thus, the inherent water splitting properties of cocatalysts are easily assessable and a complicated synthesis of a photon absorber material consisting of mixed metal oxides are avoided.[11] However, it has to be noted that Ga_2O_3 is not a suitable photon absorber material for an economical large-scale H_2 production in a sunlight-assisted water splitting process due to its large band gap, but it has been shown by Domen and coworkers[12−15] that nitridation of a Ga_2O_3/ZnO mixture results in a solid solution with d^{10} configuration that is able to absorb visible light efficiently. Consequently, Ga_2O_3 with a similar d^{10} electronic configuration is representative of this class of materials. In addition, the surface composition of GaN/ZnO solid solutions closely resembles that of Ga_2O_3,[16] and hence, the evaluation of different cocatalysts properties on the photocatalytic activity for overall water might as well be performed using commercially available Ga_2O_3.

To the best of our knowledge, molybdenum and its oxides, as an abundant material,[7] have not yet been explored as cocatalysts for photocatalytic water splitting, and its application in photocatalysis has so far been restricted to applications in which Mo is incorporated into complex mixed oxide structures.[17−21] In general, Mo is used in combination with other compounds for tuning the band gap energy of a semiconductor to enable visible light absorption. As an exception, MoS_2 has been suggested as a nonnoble metal cocatalyst for hydrogen evolution on Si,[22,23] CdS,[24] TiO_2,[25] and $ZnIn_2S_4$.[26] Although MoO_x-containing mixed oxides were recently shown to be efficient oxygen evolution electrocatalysts,[27] MoO_x-containing cocatalysts for overall water splitting were reported only in our recent study about CuO_z/CrO_y cocatalysts. Therefore, this study aims at a detailed investigation of molybdenum oxide as a suitable component to design efficient cocatalysts for overall water splitting. In this study, it is shown that MoO_x itself is a suitable cocatalyst for overall water splitting. Furthermore, it is highlighted that in combination with the previously reported CuO_z/CrO_y, highly active photocatalysts for overall water splitting can be obtained. When optimal component loadings and suitable working conditions are applied, the ternary CuO_z/CrO_y/MoO_x cocatalyst outperforms even the noble metal-based material, and stable water splitting rates can be achieved.[28] In this regard, the developed CuO_z/CrO_y/MoO_x cocatalyst system represents one of the rare examples for efficient noble-metal-free water splitting. Applying a combination of gas phase μ-reactor studies to assess the cocatalyst's ability to perform the back reaction of H_2 and O_2 to water and X-ray spectroscopy techniques (X-ray photoelectron spectroscopy (XPS), X-ray absorption near edge structure spectroscopy (XANES) and extended X-ray absorption fine structure spectroscopy (EXAFS[29]), it is shown that CrO_y most likely alters the oxidation state of the cocatalyst components and stabilizes Cu(II) rather than suppresses the back reaction.

EXPERIMENTAL SECTION

Preparation of the Photocatalyst and Photocatalytic Activity Tests. For the synthesis of the photocatalysts by stepwise photodeposition and testing for water splitting, an apparatus described previously was used (Figure S1, further information in the Supporting Information).[30] $Na_2MoO_4{\cdot}2H_2O$ (Normapur), $Cu(NO_3)_2{\cdot}2H_2O$ (Sigma-Aldrich), and K_2CrO_4 (Sigma-Aldrich) were used as precursor salts. Photodeposition was performed using suspensions of Ga_2O_3 (ChemPur) in either 50 mL of methanol/550 mL of H_2O for MoO_x or 550 mL of H_2O (pure water) for subsequently deposited CrOy and CuO_x. Typical photocatalyst concentrations during the experiments were 1.7 g/L (photodeposition) and 0.55 g/L (direct water splitting). The respective Mo, Cr, and Cu concentrations can be calculated from the relevant weight percentages. For example, for 0.6 wt % Mo, 10.2 mg/L Mo (photodeposition) and 3.3 mg/L Mo (water splitting); for 0.45 wt % Cr, 2.5 mg/L Cr; and for 0.66 wt % Cu, 3.6 mg/L Cu. After photodeposition of MoO_x in methanolic solution, the suspension was filtered, and the particles were freeze-dried overnight without additional calcination.

The reductive photodeposition of Mo in the presence of methanol as a hole scavenger can be described by the following equations:

$$MoO_4^{2-}(aq) + 2e^- + 4H^+(aq) \rightarrow MoO_2(s) + 3H_2O(l)$$

$$CH_3OH(l) + 6h^+ + H_2O(l) \rightarrow 6H^+(aq) + CO_2(g)$$

Chromium and copper were photodeposited through reaction of the metal salts with the electrons created upon absorption of light, where H_2O functions as a hole scavenger:

$$2CrO_4^{2-}(aq) + 10H^+(aq) + 6e^- \rightarrow Cr_2O_3(s) + 5H_2O(l)$$

$$Cu^{2+}(aq) + 2e^- \rightarrow Cu^0(s)$$

$$H_2O(l) + 2h^+ \rightarrow 2H^+(aq) + 0.5O_2(g)$$

Note that after exposure to air and in the absence of irradiation, reductively photodeposited species may be reoxidized.

Overall water splitting experiments in the liquid phase were performed with 300 mg of catalyst dispersed in 550 mL of water. Photodeposition and water splitting experiments were performed in a homemade quartz reactor (Figure S1) using a Hg lamp (Peschel) operated at 500 W and a total irradiance of 59 mW/cm^2 (Figure S2). Overall water splitting was performed at pH = 5.5, and no significant changes in pH were observed during the course of the experiments. Detailed information about the liquid phase water splitting setup and the quantitative analysis can be found in the Supporting Information.

The ability of the different cocatalysts to perform the back reaction of H_2 and O_2 to H_2O was tested in a μ-reactor system depicted in Figure S3 and described in detail elsewhere.[31] The preparation of the reactors was performed in a similar way. In a typical experiment, the relevant currents of the different masses measured with a QMS were allowed to stabilize in an O_2/He flow. After stabilization, H_2 was introduced into the gas stream to give a H_2/O_2 ratio of 2:1. To investigate the back reaction under illumination, perodic irradiation of the photocatalysts (with a spot size of 8 mm in diameter) was performed by a low-pressure Hg lamp (8 W) with a characteristic emission line at 254 nm and an integrated irradiance of ∼2 mW/cm^2.[32]

Characterization of the Photocatalyst. For all materials prepared, the actual cocatalyst loading was determined by elemental analysis (ICP-OES for Mo and AAS for Cr and Cu). XPS measurements were carried out in an UHV setup equipped with a Gammadata-Scienta SES 2002 analyzer. The base

DOI: 10.1021/acscatal.5b01428
ACS Catal. 2015, 5, 5530−5539

pressure in the measurement chamber was 5×10^{-10} mbar. Monochromatic Al Kα (1486.6 eV; 13.5 kV; 37 mA) was used as the incident radiation, and a pass energy of 200 eV was chosen, resulting in an energy resolution better than 0.6 eV. Charging effects were compensated using a flood gun, and binding energies were calibrated on the basis of positioning the main C 1s peak at 284.8 eV, which originates from carbon contaminations.

XAS experiments were performed at the "Spline"-beamline BM25A at the ESRF (European Synchrotron Radiation Facility) in Grenoble (France). For the measurements at the Cu K edge (8979 eV), a Si(111) double-crystal monochromator was used. Because of the low Cu concentration, fluorescence mode measurements using a hyperpure seven-element Ge detector were conducted. The solid samples were prepared as wafers using BN as a binder. Several scans were averaged to achieve a good signal-to-noise ratio. XANES spectra were analyzed using the program Athena[33] performing a linear combination fit to quantify the present fractions of different oxidation states.[34]

For data evaluation, a Victoreen-type polynomial was subtracted from the spectrum to remove the background.[33,35−37] Afterward, the first inflection point was taken as energy E_0. A piecewise polynomial was used to determine the smooth part of the spectrum. It was adjusted in a way that the low-R components of the resulting Fourier transform were minimal. The background-subtracted spectrum was divided by its smoothed part, and the photon energy was converted to photoelectron wavenumber k. For evaluation of the EXAFS spectra, the resulting functions were weighted with k^3 and calculated with EXCURVE98, which works on the basis of the EXAFS function and according to a formulation in terms of radial distribution functions:[38]

$$\chi(k) = \sum_j {S_0}^2(k)\, F_j(k) \int P_j(r_j)\, \frac{e^{-2r_j/\lambda}}{k{r_j}^2} \sin[2kr_j + \delta_j(k)]\, dr_j$$

TEM investigations were performed using an image Cs corrected FEI Titan transmission electron microscope that was operated at 300 kV. Samples for TEM were prepared without the use of solvents by simply dipping the holey carbon coated copper or nickel TEM grids into the fine catalyst powder.

RESULTS AND DISCUSSION

MoO_x-Modified Ga_2O_3. MoO_x/Ga_2O_3 samples with different Mo loadings were synthesized by irradiating a methanolic solution (10% MeOH in water) containing Ga_2O_3 and $Na_2MoO_4{\cdot}2H_2O$. During the photodeposition process, H_2 evolution due to aqueous methanol reforming decreased with increasing Mo concentration in solution, probably as a result of blocking of methanol adsorption sites/hydrogen evolution sites. Elemental analysis showed a strong dependence of the actual Mo loading on the amount of Mo precursor in solution and on the duration of irradiation (Table 1).

Subsequently, MoO_x/Ga_2O_3 with actual loadings of 0.3, 0.6, and 1.2 wt % Mo were tested for overall water splitting, resulting in 189, 95, and 201 μmol O_2/h, respectively (Figure 1). Although the activity was relatively low compared with the activity previously reported for $CuO_z/CrO_y/Ga_2O_3$[10] and $Rh_xCr_{2-x}O_3/Ga_2O_3$[30] materials, a significant H_2 and O_2 production rate with a nearly stoichiometric H_2/O_2 ratio was observed for all three MoO_x/Ga_2O_3 photocatalysts. Although the slight deviation from the stoichiometric H_2/O_2 ratio might be due to residual carbon contaminations from MoO_x

Table 1. Dependence of Irradiation Time and Suspended Precursor Amount on the Actual Mo Loading Obtained during Photodeposition in Methanolic Solution[a]

theor Mo loading (wt %)	irradiation time (h)	actual Mo loading (wt %)
0.16	1	0.17
0.3	1	0.28
0.6	1	0.36
0.6	3	0.68
0.6	6	0.65
1.2	2	0.44
10	2	1.28

[a]Hg light source, 500 W.

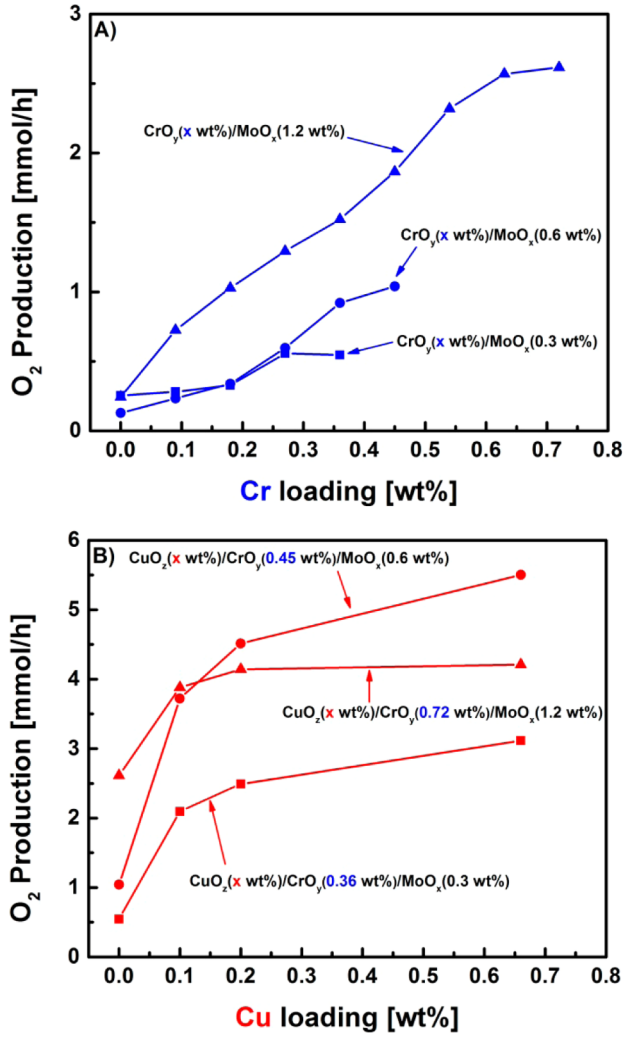

Figure 1. (A) Comparison of the water splitting activity of various Ga_2O_3 photocatalyst with varying MoO_x loadings after stepwise deposition of CrO_y from aqueous K_2CrO_4. (B) Comparison of the water splitting activity of optimized $CrO_y/MoO_x/Ga_2O_3$ photocatalyst with varying Cu loading. Squares, 0.3 wt % MoO_x; circles, 0.6 wt % MoO_x; triangles, 1.2 wt % MoO_x. For all experiments, the liquid phase water splitting system was used (Figure S1), and 300 mg of photocatalyst suspended in 550 mL pure water was irradiated with the high-pressure Hg lamp (500 W; irradiation intensity of 12.5 mW/cm^2 (250−300 nm)).

DOI: 10.1021/acscatal.5b01428
ACS Catal. 2015, 5, 5530−5539

photodeposition in methanolic solution, it can be concluded that the modification with MoO_x enables Ga_2O_3 to perform overall water-splitting under UV-light irradiation.

CrO_y/MoO_x and $CuO_z/CrO_y/MoO_x$-Modified Ga_2O_3. Because of the inherent activity of MoO_x-modified Ga_2O_3 for water splitting and the recently observed synergetic effect between CuO_z and CrO_y,[10] binary CrO_y/MoO_x- and ternary $CuO_z/CrO_y/MoO_x$-modified Ga_2O_3 photocatalysts were prepared to investigate the synergetic effects between CrO_y and CuO_z/CrO_y with MoO_x-modified Ga_2O_3 photocatalysts.

Therefore, MoO_x-modified Ga_2O_3 photocatalysts with three different MoO_x loadings were subsequently modified by CrO_y employing the previously described photodeposition procedure.[10] The photodeposition was performed in pure water, and the activity for overall water splitting was monitored directly. The subsequent photodeposition steps were performed in the absence of methanol as a sacrificial agent because MoO_x/Ga_2O_3 was already active in the overall water-splitting reaction. Thus, it was possible to monitor the effect of Cr and Cu on the photocatalytic activity of the material directly by measuring the H_2/O_2 evolution rates.

Interestingly, the photodeposition of CrO_y resulted in a further improvement of the MoO_x/Ga_2O_3 system, and a stepwise increase in water splitting activity with CrO_y loading was observed (Figure 1). The optimal Cr loading was found to increase with increasing MoO_x loading, and a CrO_y loading of 0.27 wt % for 0.3 wt % MoO_x/Ga_2O_3, 0.45 wt % for 0.6 wt % MoO_x/Ga_2O_3, and 0.72 wt % for 1.2 wt % MoO_x/Ga_2O_3 were determined to result in the highest water splitting activities, almost resembling the activity of the previously reported $CuO_z/CrO_y/Ga_2O_3$ system (Table 2).[10]

Subsequently, $CuO_z/CrO_y/MoO_x$-modified Ga_2O_3 materials were synthesized employing the optimized $CrO_y/MoO_x/Ga_2O_3$ photocatalysts. Although the addition of CuO_z to MoO_x/Ga_2O_3 materials negatively affects its overall water splitting activity (Figure S5), a positive influence of CuO_z on $CrO_y/MoO_x/Ga_2O_3$ photocatalysts was observed (Figure 1), supporting the conjecture that CrO_y is essential to enable CuO_z-based cocatalysts to split water.[10]

The optimal CuO_z loading was found to amount to 0.66 wt % for all $CrO_y/MoO_x/Ga_2O_3$ photocatalysts studied, which is in good agreement with our previous report on $CuO_z/CrO_y/Ga_2O_3$.[10] Thus, with these CuO_z loadings, highly active oxidic ternary cocatalysts on Ga_2O_3 for overall water splitting were obtained that achieved initial H_2 evolution rates as high as 42 mmol $H_2/g_{cat}/h$ for the $CuO_z/CrO_y/MoO_x$ (0.6 wt %)$/Ga_2O_3$ photocatalyst with an irradiance of 12.5 mW/cm^2 (wavelength range 250−300 nm).[39] The initial water splitting rate of an optimized nonnoble metal $CuO_z/CrO_y/MoO_x/Ga_2O_3$ system is, therefore, clearly exceeding the activity of the most active noble metal $Rh_xCr_{2-x}O_3/Ga_2O_3$ photocatalyst (Table 2).[30] In addition, with the prepared oxidic ternary $CuO_z/CrO_y/MoO_x/Ga_2O_3$ photocatalyst, hydrogen evolution rates are achieved that resemble at least the hydrogen evolution rates obtained with NiO-modified La-doped $NaTaO_3$ and RhO_x/CrO_y-modified GaN/ZnO, which to the best of our knowledge are the highest water splitting rates reported so far.[40−42] A comparison with the values reported in the literature seems reasonable because the materials were measured under similar illumination conditions; for example, an inner irradiation cell with a high-pressure Hg lamp in pure distilled water (pH not further specified). Indeed, $Rh_xCr_{2-x}O_3$-modified Ga_2O_3 previously reported from our lab[30] and used for comparison in this study exhibits activities similar to $Rh_xCr_{2-x}O_3$-modified Ga_2O_3 photocatalysts reported from other laboratories.[43] Therefore, the prepared composite material consisting of a nonnoble metal oxidic ternary $CuO_z/CrO_y/MoO_x$ cocatalyst on Ga_2O_3 can be considered highly active.

Table 2. Comparison of the Overall Water Splitting Activity of Optimized $CuO_z/CrO_y/MoO_x/Ga_2O_3$, $CuO_z/CrO_y/Ga_2O_3$, and $Rh_xCr_{2-x}O_3/Ga_2O_3$ Catalysts after Photodeposition and Treatment in Air Performed with 300 Mg of Photocatalyst Suspended in 550 mL Pure H_2O after Different Times on Stream (TOS)[a]

activity	H_2 (%)	O_2 (%)	H_2 (mmol/h)	O_2 (mmol/h)
$CuO_x/CrO_y/MoO_z/Ga_2O_3$				
0.3 wt % Mo				
initial	4.3	2.1	6.2	3.2
after 300 min TOS	1.3	0.7	1.8	0.9
after reactivation in air for 24 h	3.6	1.8	5.1	2.5
0.3 wt % Mo (after treatment in air for 24 h at RT)				
initial	4.2	2.1	6.0	3.0
after 300 min TOS	3.1	1.6	4.4	2.2
0.6 wt % Mo (after treatment in air for 24 h at RT)				
initial	10.6	5.4	16.9	8.6
after 300 min TOS	8.0	4.0	12.2	6.1
after 600 min TOS	2.2	1.1	3.0	1.5
after 900 min TOS	2.1	1.0	2.9	1.4
1.2 wt % Mo (after treatment in air for 24 h at RT)				
initial	5.3	2.9	7.7	4.3
after 300 min TOS	5.0	2.6	7.2	3.8
after 600 min TOS	3.8	2.0	5.4	2.8
$Rh_xCr_{2-x}O_3/Ga_2O_3$				
initial	5.5	2.9	8.0	4.3
after 300 min TOS	3.8	2.0	5.4	2.8
after 600 min TOS	3.0	1.6	4.2	2.2
$CuO_z/CrO_y/Ga_2O_3$				
initial	3.0	1.5	4.2	2.1
after 300 min TOS	1.5	0.8	2.1	1.1
after 600 min TOS	1.2	0.6	1.6	0.8

[a]The suspensions were irradiated with a Hg lamp operated at a power of 500 W. The total incident light intensity was measured with an actinometer (59 mW/cm^2). The portion of light containing photons with the appropriate wavelength (i.e., photons that can be absorbed by Ga_2O_3) was estimated using the spectrum of the light source. Thus, an irradiance of 12.5 mW/cm^2 was obtained. The corresponding photon flux estimating an irradiated area of 342 cm^2 was calculated to be 9.4 × 10^{-6} mol/s, equal to 34.0 mmol/h.

A gradual decrease in the activity comparable to the decrease in activity observed for $CuO_z/CrO_y/Ga_2O_3$ and $Rh_xCr_{2-x}O_3/Ga_2O_3$ (Table 2) was observed for the ternary MoO_x-based systems during prolonged time on-stream (TOS). However, a rather sudden drop in activity occurred after prolonged irradiation (Figure 2). Although the stability appeared to be better for $CuO_z/CrO_y/MoO_x/Ga_2O_3$ photocatalysts with higher MoO_x loading, the stabilized activity of all materials closely resembled the activity of the recently reported $CuO_z/CrO_y/Ga_2O_3$[10] (Table 2).

In general, deactivation phenomena in photocatalysis are often related to the occurrence of photocorrosion. Recently, $CuRhO_2$ photocathodes were reported to deactivate severely as a result of photoreduction, which was found to be reversible by treatment with air in ambient conditions or performing

DOI: 10.1021/acscatal.5b01428
ACS Catal. 2015, 5, 5530−5539

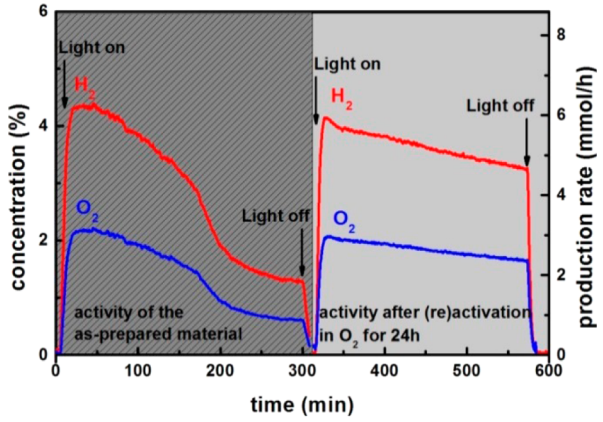

Figure 2. Overall water splitting activity in liquid phase water splitting of $CuO_z/CrO_y/MoO_x$ (0.3 wt %)/Ga_2O_3 (300 mg suspended in 550 mL pure water) directly after synthesis of the photocatalyst and after activation of the catalyst by treatment in air in an open reactor for 12 h.

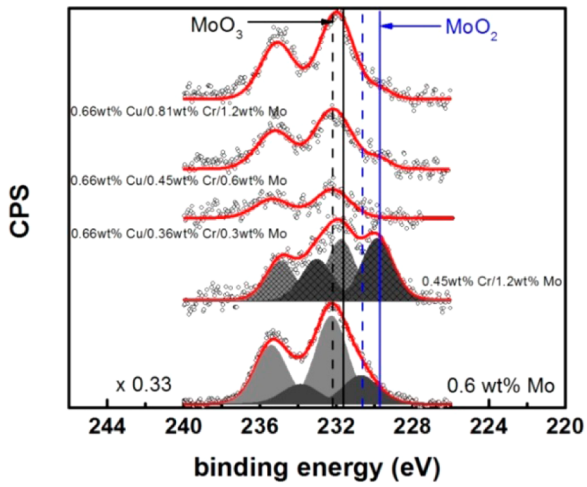

Figure 3. X-ray photoelectron Mo 3d region spectra of Ga_2O_3 photocatalysts after photodeposition of different cocatalysts. The spectra are normalized by the Ga_2O_3 O 1s signal.

photoelectrochemical hydrogen evolution in the presence of air.[44] Therefore, we tried to regenerate our system, and indeed, the photocatalyst was almost fully regenerated after extended air exposure of the suspended catalyst under ambient conditions (Table 2). Furthermore, after regeneration of the $CuO_z/CrO_y/MoO_x$ (0.3 wt %)/Ga_2O_3 photocatalyst, the material appeared to be more stable during prolonged irradiation compared with the as-prepared sample (Table 2). In addition, it was possible to prevent the deactivation and to improve the catalyst stability by performing overall water splitting in an O_2-containing carrier gas (1% O_2/N_2) (Figure S6). Thus, water splitting in the presence of O_2 is an alternative approach to the prolonged air treatment after deactivation. Moreover, the presence of O_2 in the carrier gas did not interfere with the activity, indicating that the backward reaction of H_2 and O_2 to H_2O is at least of zero order in the oxygen partial pressure at relevant oxygen pressures.

Characterization of Cocatalyst-Modified Ga_2O_3. Characterization of the different cocatalysts was performed by means of UV−vis spectroscopy (Figure S7), different X-ray spectroscopy methods, and TEM measurements. From UV−vis spectroscopy, a band gap of 4.6 eV was estimated for pure Ga_2O_3. Upon loading with MoO_x, a tailing into the visible light region extending to 450 nm was observed. This additional absorption can be attributed to the presence of MoO_3 species.[45] In Figure 3, the X-ray photoelectron spectra of the Mo 3d region of the three different $CuO_z/CrO_y/MoO_x$ cocatalysts with optimized Cu and Cr loadings are shown subsequent to transfer in air. Furthermore, two reference samples that were either MoO_x- or CrO_y/MoO_x-modified Ga_2O_3 photocatalysts are included. It is evident from the presented spectra that Mo appears to be present in the oxidation state 6+, as in MoO_3. However, the peaks are slightly asymmetric, pointing toward lower Mo oxidation states. Interestingly, Mo appears to be present in a reduced oxidation state upon addition of CrO_y (present in the III+ oxidation state (Figure S8)[10]), in which a large fraction of MoO_x is present in a MoO_2-like form with a IV + oxidation state. The oxidation state of Cr(III) was additionally confirmed by X-ray emission and high-energy resolution XANES spectroscopy (Figure S12). Furthermore, the integrated peak area of the Mo 3d signal of the CrO_y/MoO_x cocatalyst compared with the MoO_x cocatalyst is significantly smaller, although the Mo loading is almost twice for the CrO_y/MoO_x cocatalysts, as shown by elemental analysis.

It has to be noted that all spectra are normalized to the Ga_2O_3 O 1s peak, rendering them directly comparable. Therefore, it can be assumed that CrO_y is deposited mainly on the predeposited MoO_x species. Upon addition of CuO_z to the CrO_y/MoO_x-modified Ga_2O_3, the features corresponding to the low oxidation state Mo species (as in MoO_2) almost completely disappear. This phenomenon occurred for all three $CuO_z/CrO_y/MoO_x$ cocatalysts tested. In contrast, the intensity of the features corresponding to Mo with an oxidation state of 6+, as in MoO_3, appears to be unchanged when samples with similar Mo loadings are compared. Similarly, there is a decrease in intensity of the Cr $2p_{3/2}$ peak upon addition of CuO_z (Figure S8), pointing to the deposition of CuO_z onto CrO_y in the $CuO_z/CrO_y/MoO_x$ cocatalysts. Finally, the Cu_{LVV} Auger and the Cu 2p peaks analysis revealed that Cu was present mainly as Cu_2O, and Cu in higher oxidation states is present in samples with higher Mo and Cr loadings (Figures S8, S9). This is in good agreement with the oxidation state of Cu in previously reported CuO_z/CrO_y cocatalysts.[10] Nevertheless, it has to be noted that the oxidation states may change under reaction conditions in the presence of liquid water and evolving H_2 and O_2, and restructuring of the $CuO_z/CrO_y/MoO_x$ cocatalyst may occur as a result of oxidative photocorrosion and subsequent reductive photodeposition.

X-ray absorption spectroscopy was applied to investigate the photocatalysts after filtration and drying.

The XANES spectra of all samples were analyzed using a linear combination XANES fit[46] with the references bulk Cu(0), Cu(II)Ga_2O_4,[47,48] Cu(II)O,[49] and Cu(I)$_2$O[50] (Table 3, Figure S10). All four components were necessary to achieve a good fit. All possible combinations were tested, but fits with less than the four components were of inferior quality, also when taking the reduced number of floating parameters into account. The only exception is $CuO_z/CrO_y/Ga_2O_3$ (fresh), in which no Cu_2O was found in the fit. In this sample, the main component was Cu(II)Ga_2O_4, with 51 mol % Cu(0), followed by Cu(II)O, with 30%. Interestingly, Cu(0) is present here at 19.1%. The fraction of Cu(0) increases in $CuO_z/CrO_y/Ga_2O_3$ (after 10 h TOS) to almost 31%, but is reduced in $CuO_z/CrO_y/MoO_x/Ga_2O_3$ (after 15 h TOS) to 15.5%. CuO_z/Ga_2O_3 shows the

DOI: 10.1021/acscatal.5b01428
ACS Catal. 2015, 5, 5530−5539

Table 3. Results of the Linear Combination XANES Fit for Different Photocatalysts

sample	Cu^0	$CuGa_2O_4$	CuO	Cu_2O
0.66 wt % CuO_z/Ga_2O_3 (fresh)	0.561	0.185	0.058	0.196
0.66 wt % CuO_z/0.09 wt % CrO_y/Ga_2O_3 (fresh)	0.191	0.508	0.301	0
0.66 wt % CuO_z/0.09 wt % CrO_y/Ga_2O_3 (after 10 h TOS)	0.308	0.345	0.159	0.188
0.66 wt % CuO_z/0.45 wt % CrO_y/0.6 wt % MoO_x/Ga_2O_3 (after 15 h TOS)	0.155	0.459	0.244	0.143

largest amount of Cu(0), with 56.1%. The Cu(I)$_2$O content in these three samples is comparable, with values between 14.3 and 18.8%; however, the fractions of Cu(II)Ga_2O_4 and Cu(II)O differ significantly, with values of 34.5 and 15.9% for CuO_z/CrO_y/Ga_2O_3 (after 10 h TOS), 45.9 and 24.4% for CuO_z/$CrO_y/MoO_x/Ga_2O_3$ (after 15 h TOS), and 18.5 and 5.8% for CuO_z/Ga_2O_3 (fresh). The results of the XANES analysis are reflected in the EXAFS results and are presented in the Supporting Information (Figures S10, S11 and Table S1).

The used β-Ga_2O_3 support consists of rods with a porous structure and a rectangular cross section. The TEM analysis of $CuO_z/CrO_y/MoO_x/Ga_2O_3$ after 15 h TOS (Figure 4a) revealed the presence of raft-like deposits, which can be identified more clearly in the HAADF-STEM image (Figure 4b). EDX analyses of these deposits reveal that they consist of Cu, Cr, and Mo, as shown in Figure 4. In addition, a few spherical particles containing a Cu core and a shell containing Cr and Mo (Figure 4; EDX 3, 4, and 5) were detected. In view of the XPS and XAS results, these core−shell particles may originate from the deactivation of the ternary cocatalyst by reduction of CuO_z, resulting in the segregation into a Cu-rich core and a Mo- and Cr-rich shell.

Gas-Phase μ-Reactor Measurements: On the Role of the of H_2 and O_2 Backward Reaction. The synergetic effects observed between MoO_x and CrO_y in the binary cocatalyst and MoO_x, CrO_y, and CuO_z on the rate of overall water splitting is rather unclear. One of the common suggestions for the improvement in water splitting activity is the prevention of the backward reaction of H_2 and O_2 to water.[9] Indeed, CrO_y seems to hinder the backward reaction for Rh-loaded systems (and to a lower extent, for Pt-loaded systems).[31] However, the characterization results and the observation that the presence of O_2 in the carrier gas did not interfere with the water splitting rate suggests that the influence of CrO_y is not fully explained by the negligible backward reaction for the $CuO_z/CrO_y/MoO_x$ (0.3 wt %)/Ga_2O_3 photocatalyst. Therefore, a more detailed investigation of the ability of cocatalysts to catalyze the backward reaction of H_2 and O_2 was performed in the dark and under irradiation in a gas phase μ-reactor (Figure 5),[51,52] which was recently shown to be an appropriate approach to study this reaction.[31,53]

In a first attempt, the μ-reactor was thoroughly purged in a O_2/He gas stream to achieve a low baseline for the water signal (m/e (18)). After stabilization of the signals, the different photocatalysts were irradiated by chopped light using a Hg lamp (Figure 5A, 0−30 min). A decrease in the water signal was observed for Cr (0.09 wt %)/Rh (0.1 wt %)- and $CuO_z/CrO_y/MoO_x$ (0.3 wt %)-modified Ga_2O_3 photocatalysts, whereas a slight increase in the H_2O signal was detected for Rh (0.1 wt %)-, Cu (0.66 wt %)-, and Cu (0.66 wt %)/Cr (0.09 wt %)-modified Ga_2O_3 (Figure 5A). The decrease in H_2O signal for Cr (0.09 wt %)/Rh (0.1 wt %)- and $CuO_z/CrO_y/MoO_x$ (0.3 wt %)-modified Ga_2O_3 photocatalysts can be attributed to the light-driven splitting of traces of water present in the gas stream or adsorbed on the photocatalyst surface, which was confirmed by a simultaneously increasing H_2 signal. On the other hand, the slight increase in the H_2O signal for the other inherently less active materials might be attributed to the light-induced desorption of traces of water from the catalyst surface. This result underlines the high activity of the $CuO_z/CrO_y/MoO_x$ (0.3 wt %)/Ga_2O_3 for water splitting. Subsequently, H_2 was introduced into the gas stream to create a H_2- and O_2-

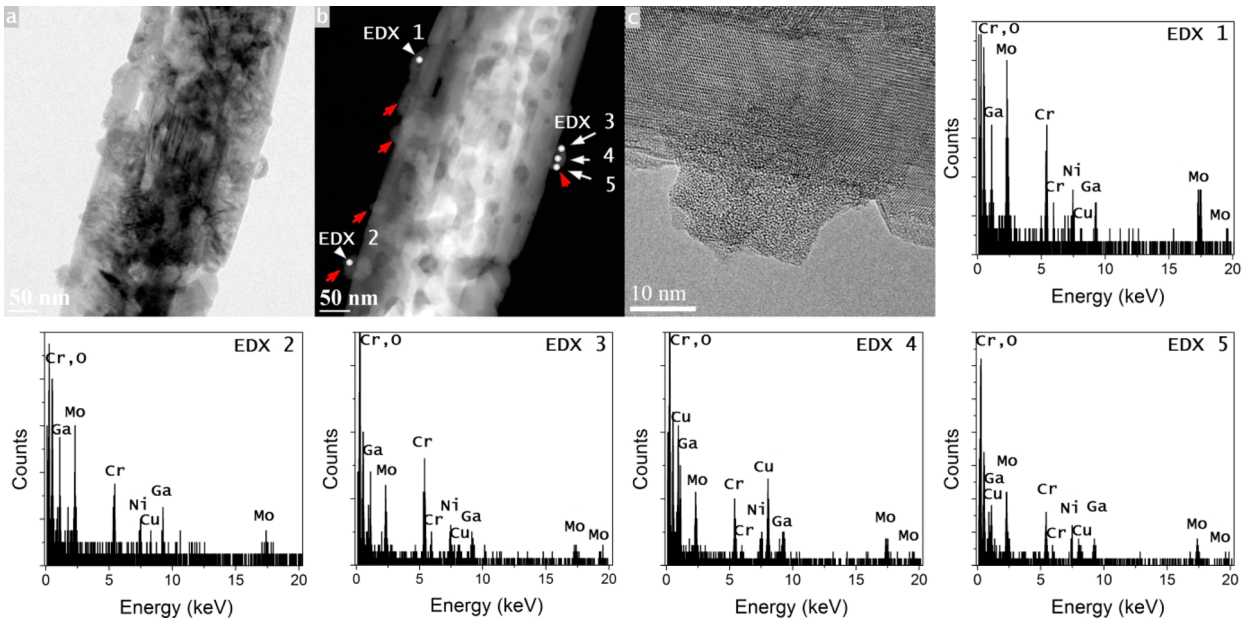

Figure 4. (a) Bright-field TEM image and (b) dark-field STEM image of 0.66 wt % CuO_z/0.45 wt % CrO_y/0.6 wt % MoO_x/Ga_2O_3 (after 15 h TOS). Surface decorations are indicated by red arrows. (c) HRTEM image of an amorphous surface deposit. EDX spectra recorded from the indicated regions in part b reveal slightly varying compositions of the Cu-, Cr-, and Mo-containing deposits. Ni peaks originate from the Ni TEM grid.

DOI: 10.1021/acscatal.5b01428
ACS Catal. 2015, 5, 5530−5539

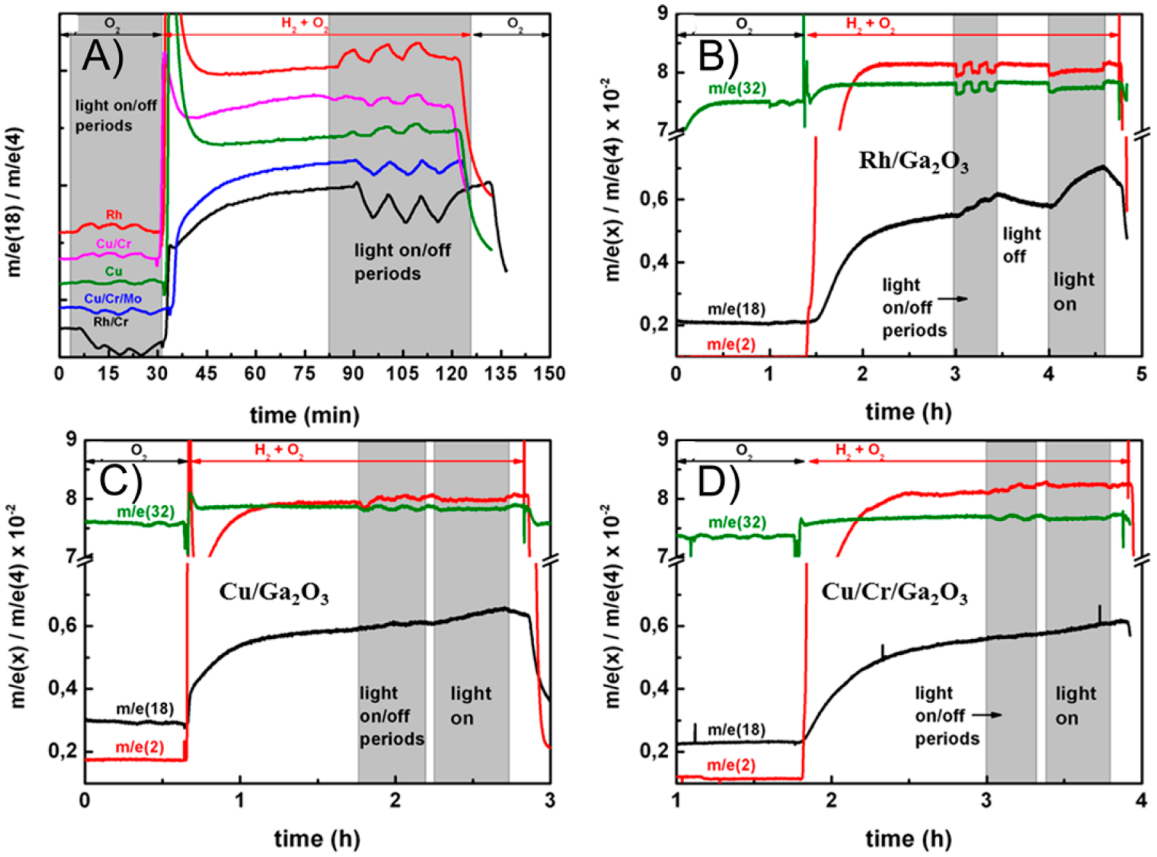

Figure 5. (A) Back reaction of H_2 and O_2 performed in a gas phase μ-reactor at 298 K for different cocatalyst systems. Rh (0.1 wt %)/Ga_2O_3, Cu (0.66 wt %)/Cr (0.09 wt %)/Ga_2O_3, Cu (0.66 wt %)/Ga_2O_3, $CuO_z/CrO_y/MoO_x$ (0.3 wt %)/Ga_2O_3, and Cr (0.09 wt %)/Rh (0.1 wt %)/Ga_2O_3 were used. The H_2O signal (m/e (18)) was measured upon exposing the catalyst to a mixture of H_2 and O_2 in a stoichiometric ratio with and without light irradiation as indicated. The current of the water signal in these experiments, which is representative for the water concentration, was on the order of 1 nA, corresponding to 8.78×10^{12} molecules/s of water at the beginning of these experiments. (B–D) Back reaction of H_2 and O_2 performed in a gas phase μ-reactor at 298 K for different cocatalyst systems with low residual water (10 times lower compared with panel A content in the gas stream. The H_2O signal (m/e (18)) was measured upon exposing the catalyst to a mixture of H_2 and O_2 in a stoichiometric ratio with and without light irradiation as indicated for (B) Rh(wt %)/Ga_2O_3, (C) Cu(0.66 wt %)/Ga_2O_3, and (D) Cu (0.66 wt %)/Cr (0.09 wt %)/Ga_2O_3.

containing gas mixture in He as carrier gas. A gradual increase of the m/e (18) signal was observed when Cr (0.09 wt %)/Rh (0.1 wt %)/Ga_2O_3 and $CuO_z/CrO_y/MoO_x$ (0.3 wt %)/Ga_2O_3 photocatalysts were in the reactor (Figure 5A, 30–80 min). A similar increase was also observed with a blank reactor, which is therefore attributed to the reaction of H_2 and O_2 to H_2O at the QMS filament (Figure S13). Eventually, the signal reached a constant value similar in intensity for all materials as well as for the blank reactor. Therefore, it can be concluded that the back reaction under steady state conditions in the dark is small for all materials. Under irradiation (Figure 5A, 80–125 min), even in the presence of H_2 and O_2, water splitting rather than the backward reaction was observed for Cr (0.09 wt %)/Rh (0.1 wt %)- and $CuO_z/CrO_y/MoO_x$ (0.3 wt %)-modified Ga_2O_3 photocatalysts. For the Cu-containing photocatalysts (Figure 5A, green and purple trace), a slight increase in the m/e (18) signal was observed, and only in the case of the Rh (0.1 wt %)-modified Ga_2O_3 (Figure 5A, red trace) was a pronounced increase in the m/e (18) signal detected. Thus, it can be concluded that only bare Rh catalyzes the water formation of water from H_2 and O_2 to a significant extent, which is in agreement with earlier findings.[31] For the other cocatalysts, this back reaction was insignificant, and in the case of the intrinsically most active materials ($CuO_z/CrO_y/MoO_x$ (0.3 wt %)- and Cr (0.09 wt %)/Rh (0.1 wt %)-modified Ga_2O_3), splitting of even small traces of water was observed. Thus, a contribution of MoO_x to the back reaction is unlikely, and only the ability of CuO_z remained unclear.

Additional experiments were performed with a lower water content (QMS current of 0.1 nA for m/e (18) after stabilization corresponding to 8.78×10^{11} molecules/s) with Rh (0.1 wt %)-, Cu (0.66 wt %)-, and Cu (0.66 wt %)/Cr (0.09 wt %)-modified Ga_2O_3 photocatalysts to further investigate Cu-containing cocatalysts. As shown in Figure 5B–D, again only for Rh (0.1 wt %)-modified Ga_2O_3 (Figure 5B) was a significant increase in the water signal m/e (18) due to the occurrence of the back reaction observed. On the contrary, neither with Cu (0.66 wt %) (Figure 5C), nor with Cu (0.66 wt %)/Cr (0.09 wt %) (Figure 5D) cocatalysts is the back reaction of H_2 and O_2 to H_2O occurring to a significant extent. Thus, the conjecture that O_2 in the carrier gas (Figure S6) is not interfering with the water splitting activity of $CuO_z/CrO_y/MoO_x$ (0.3 wt %)/Ga_2O_3 is confirmed by the photocatalytic measurements of the backward reaction in the gas phase (Figure 5A). Accordingly, since the presence of CrO_y renders all CuO_z-modified Ga_2O_3 active for water splitting, it is concluded that CrO_y in this system alters the intrinsic properties of the CuO_z cocatalyst, enabling the forward water splitting reaction rather than suppressing the back reaction.

DOI: 10.1021/acscatal.5b01428
ACS Catal. 2015, 5, 5530–5539

DISCUSSION

Remarkably, photodeposited MoO_x enabled Ga_2O_3 to split water into H_2 and O_2 under UV irradiation. Although Ga_2O_3 is known to be a suitable photon absorber for water splitting upon cocatalyst modification, so far, the ability to render Ga_2O_3 active was restricted mainly to noble-metal-containing cocatalysts[43] and the nonnoble-metal systems NiO[54] and CuO_z/CrO_y.[10] Particularly, this observation is interesting because it has been previously shown that only CuO_z- or CrO_y-modified Ga_2O_3 catalysts were hardly active for the overall water splitting under UV light irradiation.[10] Instead, for the MoO_x-containing systems, the photocatalytic activity was even further increased upon addition of CrO_y and CuO_x. Thus, a ternary cocatalyst that outperforms even the noble metal $Rh_xCr_{2-x}O_3$ cocatalyst system was obtained.

The obtained characterization results show that the ternary $CuO_z/CrO_y/MoO_x$ cocatalyst is present in a layered-like structure that originates from the applied sequential photodeposition of the three components (Figure 6).

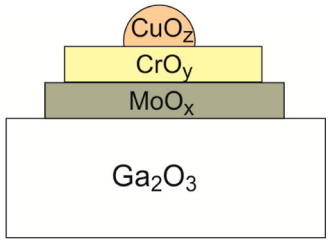

Figure 6. Schematic representation of the cocatalyst structure obtained by sequential photodeposition.

XPS results indicate that MoO_x in the bottom layer is present in the highest possible oxidation state, even though the photodeposition is a reductive process. However, in situ characterization is certainly required to confirm these oxidation states because the sample is exposed to air after photodeposition during the transfer to the XPS setup. Moreover, the observation that the CrO_y loading at which the highest water splitting activity for CrO_y/MoO_x-modified Ga_2O_3 is achieved increases concomitantly with increasing MoO_x loading points to a close interaction between CrO_y and MoO_x. This conclusion is confirmed by the XPS results showing that MoO_x is shielded by the deposited CrO_y. The accompanying partial reduction of Mo^{6+} during the reductive photodeposition of CrO_y indicates again a close interaction between MoO_x and CrO_y enabling charge transfer. A similar observation was recently reported for Cr-modified MoS_2, in which Cr nanoparticles have been shown to enhance the H_2 evolution rate and stability of MoS_2,[55] which is in good agreement with our observations for the MoO_x cocatalyst shown here.

In our previous report on CuO_z/CrO_y-modified Ga_2O_3 photocatalysts[10] it was shown that dosing of a small amount of Cr (0.09 wt %) to CuO_z/Ga_2O_3 is necessary, though sufficient to enable the photocatalyst to perform overall water splitting in the liquid phase. Instead, for MoO_x, the optimal CrO_y increased with MoO_x loading. Even though the role of MoO_x in water splitting is not fully understood (OER or HER catalyst), the partial reduction of MoO_x observed by XPS indicates that MoO_2 rather than is MoO_3 is the active component in water splitting. This is in line with the fact that Mo in $Fe_2(MoO_4)_3$, which can be used as OER catalysts, is present as Mo^{4+}.[27]

Nevertheless, the observation that only small amounts of Cr are sufficient to enable Cu to be a cocatalyst for water splitting is important for rationalizing the increase in activity of the Cu-containing $CuO_z/CrO_y/MoO_x$ system. For $CuO_z/MoO_x/Ga_2O_3$, a decrease in activity was observed with increasing Cu loading (Figure S5), whereas CrO_y in CuO_z/CrO_y-modified Ga_2O_3 is beneficial for the water splitting activity. Hence, the presence of CrO_y, rather than MoO_x, is crucial to enable CuO_z to be an active cocatalyst component in overall water splitting. This difference can be explained mostly by different oxidation states of copper in the $CuO_z/MoO_x/Ga_2O_3$ and $CuO_z/CrO_y/Ga_2O_3$ systems. Indeed, from XANES and EXAFS measurements, it can be concluded that the presence of CrO_y even in very small amounts strongly influences the oxidation state of copper.

In the absence of CrO_y, the sample is hardly active for water splitting, and the main part of Cu in the fresh sample is present in the metallic state even after storage under atmospheric conditions. In the presence of CrO_y, however, the main part of Cu in the fresh sample is present as Cu(II). During irradiation under water splitting conditions, the fraction of metallic copper increases, as shown by comparing the fresh sample with the sample after 10 h TOS at the expense of the fraction of Cu(II). When taking into account that the catalyst is deactivating under reaction conditions, it is concluded that the presence of highly oxidized Cu(II) is an indispensable component of an active catalyst Cu-containing cocatalyst, which is in good agreement with recent studies of CuO_x/Nb_2O_5.[56] In addition, copper-based systems are known to suffer from photodegradation in solution.[57−59] However, Cu oxides can be stabilized by CrO_y, particularly in structures such as delafossite ($CuCrO_2$)[60] or spinel ($CuCr_2O_4$),[61] which is also in good agreement with our recent report on photocatalytic activity for overall water splitting of CuO_z/CrO_y-modified Ga_2O_3.[10] Therefore, it is likely that the increase in the photocatalytic behavior of the $CrO_y/MoO_x/Ga_2O_3$ (Figure 1) upon addition of CuO_z can also be explained by the stabilization of Cu(II) in the ternary systems.

Obviously, the presence of MoO_x itself is not sufficient to stabilize Cu(II), but in the ternary $CuO_z/CrO_y/MoO_x$ cocatalyst, it is evident from the XANES and EXAFS results that even after a long time on stream, only small fractions of metallic copper were detected in the ternary $CuO_z/CrO_y/MoO_x$ cocatalyst and a relatively high fraction of Cu(II) remained, whereas in CuO_z/CrO_y-modified Ga_2O_3, copper was already reduced to a larger extent (Table 3). Clearly, in the presence of MoO_x, the reduction of Cu(II) during irradiation is further inhibited. Therefore, the abrupt deactivation of the ternary $CuO_z/CrO_y/MoO_x$ cocatalysts, especially at low Mo-loadings (0.3 wt %), cannot be attributed to the reduction of CuO_x. Instead, the results suggest that MoO_x rather than CuO_z is photoreduced to some inactive state during long-term water splitting and that the oxidation by treatment in air reoxidizes MoO_x. This conjecture is in line with slower degradation rates observed for catalysts with higher Mo loadings and with water splitting rates of the deactivating $CuO_z/CrO_y/MoO_x$ cocatalysts approaching those of a similar CuO_z/CrO_y cocatalyst system (Table 2).

Finally, measurements of the back reaction of H_2 and O_2 reveal that all nonnoble metal cocatalysts studied here barely enable the formation of water, either in the dark or under irradiation. The suppression of the back reaction by the formation of a chromia shell, however, is usually reported to be

DOI: 10.1021/acscatal.5b01428
ACS Catal. 2015, 5, 5530−5539

key to enable overall water splitting for noble metal, for example, Rh-modified photocatalysts.[30] This was also observed in this study, though to a lower extent because of rather small loadings, for Rh-modified Ga_2O_3. Although the function of each component in the ternary $CuO_z/CrO_y/MoO_x$ cocatalysts has to be further explored, the characterization results obtained here in combination with the minor tendency to promote the backward reaction of water indicate that CrO_y rather than just blocking the back reaction is beneficial in multiple processes promoting water splitting, at least for the nonnoble metal cocatalysts reported here.

Although the results here obtained certainly open up the possibility to design a noble-metal-free photocatalyst for overall water splitting, the deposition of the ternary cocatalyst on a visible-light-active semiconductor is certainly required. Furthermore, monitoring of the changes in the oxidation states by in situ techniques such as X-ray absorption spectroscopy is currently under investigation, which will guide further research to stabilize the system for long-term operation, focusing on high-temperature O_2 treatments, water splitting in different pH regimes, and maintaining the active MoO_x phase.

CONCLUSIONS

A ternary noble-metal-free cocatalyst has been developed enabling Ga_2O_3 to perform efficient photocatalytic water splitting under UV irradiation. The novel cocatalyst consisting of CuO_z, CrO_y and MoO_x was obtained by stepwise photodeposition on Ga_2O_3, resulting in activities that are at least comparable to the noble-metal-containing $Rh_xCr_{2-x}O_3/Ga_2O_3$ system. X-ray-based characterization techniques and TEM revealed that the cocatalyst is present in a layered structure. Both CrO_y and MoO_x were found to stabilize CuO_z against reduction. The observed deactivation can be either reversed or prevented by a treatment with O_2, leading to a stable photocatalytic performance while maintaining high water splitting rates. The investigation of the back reaction in the gas phase revealed that CrO_y is not simply blocking the backward reaction of H_2 and O_2 to water, as reported for noble-metal-containing systems. In fact, synergetic effects with MoO_x and CuO_z were observed, enabling higher water splitting rates. Thus, employing ternary or even multicomponent cocatalyst systems, which are already commonly used in various heterogeneous reactions, will open up new routes for the design of efficient, low-cost photocatalysts.

ASSOCIATED CONTENT

Supporting Information

The Supporting Information is available free of charge on the ACS Publications website at DOI: 10.1021/acscatal.5b01428.

Description of the set-ups used, additional figures, and tables (PDF)

AUTHOR INFORMATION

Corresponding Author

*Fax: (+49)234-32-14115, E-mail: muhler@techem.rub.de.

Notes

The authors declare no competing financial interests.

ACKNOWLEDGMENTS

For funding, we gratefully acknowledge the Danish National Research Foundation's Center for Individual Nanoparticle Functionality (DNRF54) and the Mercator Research Center Ruhr (MERCUR Pr-2012-0053). M.B. kindly acknowledges provision of beamtime at the ESRF (Grenoble) as well as financial support by the Bundesministerium für Bildung and Forschung in frame of the projects SusXES and SusChEmX. B.M. acknowledges funding from the Ruhr-University Research School Plus (Gateway Fellowship). D. B. Trimarco and M. G. Nielsen are acknowledged for supporting the μ-reactor measurements. M.B. thanks the synchrotron ESRF and the beamlines BM25 A and ID26 for provision of beamtime. Funding by the BMBF in frame of the project SusChEmX is also acknowledged by M.B.

REFERENCES

(1) Tsuji, I.; Kato, H.; Kudo, A. *Chem. Mater.* **2006**, *18*, 1969−1975.
(2) Kominami, H.; Nishimune, H.; Ohta, Y.; Arakawa, Y.; Inaba, T. *Appl. Catal., B* **2012**, *111*−*112*, 297−302.
(3) Pal, B.; Torimoto, T.; Okazaki, K.; Ohtani, B. *Chem. Commun. (Cambridge, U. K.)* **2007**, No. 5, 483−485.
(4) Shen, P.; Zhao, S.; Su, D.; Li, Y.; Orlov, A. *Appl. Catal., B* **2012**, *126*, 153−160.
(5) Chen, D.; Ye, J. *Chem. Mater.* **2009**, *21*, 2327−2333.
(6) Takata, T.; Domen, K. *J. Phys. Chem. C* **2009**, *113*, 19386−19388.
(7) Vesborg, P. C. K.; Jaramillo, T. F. *RSC Adv.* **2012**, *2*, 7933−7947.
(8) Pinaud, B. a.; Benck, J. D.; Seitz, L. C.; Forman, A. J.; Chen, Z.; Deutsch, T. G.; James, B. D.; Baum, K. N.; Baum, G. N.; Ardo, S.; Wang, H.; Miller, E.; Jaramillo, T. F. *Energy Environ. Sci.* **2013**, *6*, 1983−2002.
(9) Maeda, K.; Ohno, T.; Domen, K. *Chem. Sci.* **2011**, *2*, 1362−1368.
(10) Busser, G. W.; Mei, B.; Pougin, A.; Strunk, J.; Gutkowski, R.; Schuhmann, W.; Willinger, M.-G.; Schlögl, R.; Muhler, M. *ChemSusChem* **2014**, *7*, 1030−1034.
(11) Wang, X.; Xu, Q.; Li, M.; Shen, S.; Wang, X.; Wang, Y.; Feng, Z.; Shi, J.; Han, H.; Li, C. *Angew. Chem., Int. Ed.* **2012**, *51*, 13089−13092.
(12) Maeda, K.; Teramura, K.; Takata, T.; Hara, M.; Saito, N.; Toda, K.; Inoue, Y.; Kobayashi, H.; Domen, K. *J. Phys. Chem. B* **2005**, *109*, 20504−20510.
(13) Maeda, K.; Domen, K. *Chem. Mater.* **2010**, *22*, 612−623.
(14) Yoshida, M.; Hirai, T.; Maeda, K.; Saito, N.; Kubota, J.; Kobayashi, H.; Inoue, Y.; Domen, K. *J. Phys. Chem. C* **2010**, *114*, 15510−15515.
(15) Yashima, M.; Yamada, H.; Maeda, K.; Domen, K. *Chem. Commun. (Cambridge, U. K.)* **2010**, *46*, 2379−2381.
(16) Phivilay, S. P.; Roberts, C. A.; Puretzky, A. A.; Domen, K.; Wachs, I. E. *J. Phys. Chem. Lett.* **2013**, *4*, 3719−3724.
(17) Hou, Y.; Zuo, F.; Dagg, A.; Feng, P. *Nano Lett.* **2012**, *12*, 6464−6473.
(18) Park, H. S.; Lee, H. C.; Leonard, K. C.; Liu, G.; Bard, A. J. *ChemPhysChem* **2013**, *14*, 2277−2287.
(19) Zhang, K.; Heo, N.; Shi, X.; Park, J. H. *J. Phys. Chem. C* **2013**, *117*, 24023−24032.
(20) Fu, X.; Ji, J.; Tang, W.; Liu, W.; Chen, S. *Mater. Chem. Phys.* **2013**, *141*, 719−726.
(21) Saito, K.; Kazama, S.; Matsubara, K.; Yui, T.; Yagi, M. *Inorg. Chem.* **2013**, *52*, 8297−8299.
(22) Hou, Y.; Abrams, B. L.; Vesborg, P. C. K.; Björketun, M. E.; Herbst, K.; Bech, L.; Setti, A. M.; Damsgaard, C. D.; Pedersen, T.; Hansen, O.; Rossmeisl, J.; Dahl, S.; Nørskov, J. K.; Chorkendorff, I. *Nat. Mater.* **2011**, *10*, 434−438.
(23) Laursen, A. B.; Kegnæs, S.; Dahl, S.; Chorkendorff, I. *Energy Environ. Sci.* **2012**, *5*, 5577−5591.
(24) Zong, X.; Yan, H.; Wu, G.; Ma, G.; Wen, F.; Wang, L.; Li, C. *J. Am. Chem. Soc.* **2008**, *130*, 7176−7177.
(25) Xiang, Q.; Yu, J.; Jaroniec, M. *J. Am. Chem. Soc.* **2012**, *134*, 6575−6578.
(26) Wei, L.; Chen, Y.; Lin, Y.; Wu, H.; Yuan, R.; Li, Z. *Appl. Catal., B* **2014**, *144*, 521−527.

DOI: 10.1021/acscatal.5b01428
ACS Catal. 2015, 5, 5530−5539

(27) Srirapu, V. K. V. P.; Sharma, C. S.; Awasthi, R.; Singh, R. N.; Sinha, A. S. K. *Phys. Chem. Chem. Phys.* **2014**, *16*, 7385−7393.
(28) Busser, G. W.; Mei, B.; Muhler, M. Molybdänhaltiger quaternärer Cokatalysator für die effiziente photokatalytische Wasserspaltung. German Patent 102014222816.6, 2014.
(29) Bauer, M.; Bertagnolli X-ray Absorption Spectroscopy: The Method and its Application. *Methods in Physical Chemistry*; Schäfer, R., Schmidt, P. C., Eds.; H. Wiley-VCH Verlag GmbH & Co. KGaA: Weinheim, 2012; pp 231−269.
(30) Busser, G. W.; Mei, B.; Muhler, M. *ChemSusChem* **2012**, *5*, 2200−2206.
(31) Dionigi, F.; Vesborg, P. C. K.; Pedersen, T.; Hansen, O.; Dahl, S.; Xiong, A.; Maeda, K.; Domen, K.; Chorkendorff, I. *J. Catal.* **2012**, *292*, 26−31.
(32) Vesborg, P. C. K.; Chorkendorff, I.; Brock-Nannestad, T.; Dethlefsen, J. R.; Bendix, J. *Rev. Sci. Instrum.* **2011**, *82*, 096102−3.
(33) Ravel, B.; Newville, M. *J. Synchrotron Radiat.* **2005**, *12*, 537−541.
(34) Bauer, M.; Kauf, T.; Christoffers, J.; Bertagnolli, H. *Phys. Chem. Chem. Phys.* **2005**, *7*, 2664−2670.
(35) Ertel, T.; Bertagnolli, H.; Hückmann, S.; Kolb, U.; Peter, D. *Appl. Spectrosc.* **1992**, *46*, 690−698.
(36) Newville, M. *J. Synchrotron Radiat.* **2001**, *8*, 322−324.
(37) Newville, M.; Liviņš, P.; Yacoby, Y.; Rehr, J.; Stern, E. *Phys. Rev. B: Condens. Matter Mater. Phys.* **1993**, *47*, 14126−14131.
(38) Binsted, N.; Hasnain, S. S. *J. Synchrotron Radiat.* **1996**, *3*, 185−196.
(39) Wachs, I. E.; Phivilay, S. P.; Roberts, C. A. *ACS Catal.* **2013**, *3*, 2606−2611.
(40) Kato, H.; Asakura, K.; Kudo, A. *J. Am. Chem. Soc.* **2003**, *125*, 3082−3089.
(41) Ran, J.; Zhang, J.; Yu, J.; Jaroniec, M.; Qiao, S. Z. *Chem. Soc. Rev.* **2014**, *43*, 7787−7812.
(42) Maeda, K.; Teramura, K.; Saito, N.; Inoue, Y.; Domen, K. *J. Catal.* **2006**, *243*, 303−308.
(43) Sakata, Y.; Matsuda, Y.; Nakagawa, T.; Yasunaga, R.; Imamura, H.; Teramura, K. *ChemSusChem* **2011**, *4*, 181−184.
(44) Gu, J.; Yan, Y.; Krizan, J. W.; Gibson, Q. D.; Detweiler, Z. M.; Cava, R. J.; Bocarsly, A. B. *J. Am. Chem. Soc.* **2014**, *136*, 830−833.
(45) Dieterle, M.; Weinberg, G.; Mestl, G. *Phys. Chem. Chem. Phys.* **2002**, *4*, 812−821.
(46) Bauer, M.; Heusel, G.; Mangold, S.; Bertagnolli, H. *J. Synchrotron Radiat.* **2010**, *17*, 273−279.
(47) Conrad, F.; Bauer, M.; Weyeneth, S.; Zhou, Y.; Hametner, K.; Günther, D.; Patzke, G. R. *Solid State Sci.* **2013**, *24*, 125−132.
(48) Conrad, F.; Bauer, M.; Sheptyakov, D.; Weyeneth, S.; Jaeger, D.; Hametner, K.; Car, P.-E.; Patscheider, J.; Günther, D.; Patzke, G. R. *RSC Adv.* **2012**, *2*, 3076−3082.
(49) Kirfel, A.; Eichhorn, K. *Acta Crystallogr., Sect. A: Found. Crystallogr.* **1990**, *46*, 271−284.
(50) Ene, A. B.; Bauer, M.; Archipov, T.; Roduner, E. *Phys. Chem. Chem. Phys.* **2010**, *12*, 6520−6531.
(51) Vesborg, P. C. K.; Olsen, J. L.; Henriksen, T. R.; Chorkendorff, I.; Hansen, O. *Chem.— Eng. J.* **2010**, *160*, 738−741.
(52) Vesborg, P. C. K.; In, S.; Olsen, J. L.; Henriksen, T. R.; Abrams, B. L.; Hou, Y.; Kleiman-Shwarsctein, A.; Hansen, O.; Chorkendorff, I. *J. Phys. Chem. C* **2010**, *114*, 11162−11168.
(53) Dionigi, F.; Vesborg, P. C. K.; Pedersen, T.; Hansen, O.; Dahl, S.; Xiong, A.; Maeda, K.; Domen, K.; Chorkendorff, I. *Energy Environ. Sci.* **2011**, *4*, 2937−2942.
(54) Sakata, Y.; Matsuda, Y.; Yanagida, T.; Hirata, K.; Imamura, H.; Teramura, K. *Catal. Lett.* **2008**, *125*, 22−26.
(55) Yang, L.; Zhong, D.; Zhang, J.; Yan, Z.; Ge, S.; Du, P.; Jiang, J.; Sun, D.; Wu, X.; Fan, Z.; Dayeh, S. a; Xiang, B. *ACS Nano* **2014**, *8*, 6979−6985.
(56) Furukawa, S.; Tsukio, D.; Shishido, T.; Teramura, K.; Tanaka, T. *J. Phys. Chem. C* **2012**, *116*, 12181−12186.
(57) Paracchino, A.; Mathews, N.; Hisatomi, T.; Stefik, M.; Tilley, S. D.; Grätzel, M. *Energy Environ. Sci.* **2012**, *5*, 8673−8681.
(58) Zhang, P.; Shi, Y.; Chi, M.; Park, J.-N.; Stucky, G. D.; McFarland, E. W.; Gao, L. *Nanotechnology* **2013**, *24*, 345704−345704−8.
(59) Marimuthu, A.; Zhang, J.; Linic, S. *Science* **2013**, *339*, 1590−1593.
(60) Ma, Y.; Zhou, X.; Ma, Q.; Litke, A.; Liu, P.; Zhang, Y.; Li, C.; Hensen, E. J. M. *Catal. Lett.* **2014**, *144*, 1487−1493.
(61) Xiong, D.; Xu, Z.; Zeng, X.; Zhang, W.; Chen, W.; Xu, X.; Wang, M.; Cheng, Y.-B. *J. Mater. Chem.* **2012**, *22*, 24760−24768.

DOI: 10.1021/acscatal.5b01428
ACS Catal. 2015, 5, 5530−5539